

Water Resources Research®



RESEARCH ARTICLE

10.1029/2021WR031600

Key Points:

- A new formulation for infiltration characteristic time, t_{grav} , is provided
- The reformulated t_{grav} seems to be a better criterion for convergence time of Philip's truncated infiltration equations
- The usage of reformulated t_{grav} improves predictions of soil hydraulic parameters

Correspondence to:

M. Rahmati,
mehdirmati@gmail.com;
m.rahmati@fz-juelich.de

Citation:

Rahmati, M., Latorre, B., Moret-Fernández, D., Lassabatere, L., Talebian, N., Miller, D., et al. (2022). On infiltration and infiltration characteristic times. *Water Resources Research*, 58, e2021WR031600. <https://doi.org/10.1029/2021WR031600>












Received 10 NOV 2021

Accepted 9 MAY 2022

Author Contributions:

Conceptualization: Mehdi Rahmati
Data curation: Mehdi Rahmati, Borja Latorre
Formal analysis: Mehdi Rahmati, Borja Latorre
Investigation: Mehdi Rahmati
Methodology: Mehdi Rahmati, Borja Latorre, David Moret-Fernández, Laurent Lassabatere
Resources: Mehdi Rahmati
Software: Mehdi Rahmati
Validation: Mehdi Rahmati, Borja Latorre, David Moret-Fernández, Laurent Lassabatere, Nima Talebian, Dane Miller, Renato Morbidelli, Massimo Iovino, Vincenzo Bagarello, Ying Zhao, Jan Vanderborght, Lutz Weihermüller, Rafael Angulo Jaramillo, Dani Or, Martinus Th. van Genuchten, Harry Vereecken
Visualization: Mehdi Rahmati
Writing – original draft: Mehdi Rahmati

On Infiltration and Infiltration Characteristic Times

Mehdi Rahmati^{1,2} , Borja Latorre³, David Moret-Fernández³, Laurent Lassabatere⁴, Nima Talebian⁵ , Dane Miller⁵, Renato Morbidelli⁶ , Massimo Iovino⁷ , Vincenzo Bagarello⁷ , Mohammad Reza Neyshabouri⁸, Ying Zhao⁹ , Jan Vanderborght² , Lutz Weihermüller² , Rafael Angulo Jaramillo⁴, Dani Or^{10,11} , Martinus Th. van Genuchten^{12,13} , and Harry Vereecken² 

¹Department of Soil Science and Engineering, Faculty of Agriculture, University of Maragheh, Maragheh, Iran,

²Forschungszentrum Jülich GmbH, Institute of Bio- and Geosciences: Agrosphere (IBG-3), Jülich, Germany, ³Departamento de Suelo y Agua, Estación Experimental de Aula Dei, Consejo Superior de Investigaciones Científicas (CSIC), Zaragoza, Spain, ⁴University Lyon, Université Claude Bernard Lyon 1, CNRS, ENTPE, UMR5023 LEHNA, Vaulx-en-Velin, France, ⁵Faculty of Society & Design, Bond University, Robina, QLD, Australia, ⁶Department of Civil and Environmental Engineering, University of Perugia, Perugia, Italy, ⁷Department of Agricultural, Food and Forest Sciences, University of Palermo, Palermo, Italy, ⁸Department of Soil Science and Engineering, Faculty of Agriculture, University of Tabriz, Tabriz, Iran, ⁹College of Resources and Environmental Engineering, Ludong University, Yantai, China, ¹⁰Department of Environmental Systems Science, ETH, Zurich, Switzerland, ¹¹Division of Hydrologic Sciences (DHS) - Desert Research Institute, Reno, NV, USA, ¹²Department of Earth Sciences, Utrecht University, Utrecht, The Netherlands, ¹³Center for Environmental Studies, CEA, São Paulo State University, Rio Claro, Brazil

Abstract In his seminal paper on the solution of the infiltration equation, Philip (1969), <https://doi.org/10.1016/b978-1-4831-9936-8.50010-6> proposed a gravity time, t_{grav} , to estimate practical convergence time and the time domain validity of his infinite time series expansion, TSE, for describing the transient state. The parameter t_{grav} refers to a point in time where infiltration is dominated equally by capillarity and gravity as derived from the first two (dominant) terms of the TSE. Evidence suggests that applicability of the truncated two-term equation of Philip has a time limit requiring higher-order TSE terms to better describe the infiltration process for times exceeding that limit. Since the conceptual definition of t_{grav} is valid regardless of the infiltration model used, we opted to reformulate t_{grav} using the analytic implicit model proposed by Parlange et al. (1982), <https://doi.org/10.1097/00010694-198206000-00001> valid for all times and related TSE. Our derived gravity times ensure a given accuracy of the approximations describing transient states, while also providing insight about the times needed to reach steady state. In addition to the roles of soil sorptivity (S) and the saturated (K_s) and initial (K_i) hydraulic conductivities, we explored the effects of a soil specific shape parameter β , involved in Parlange's model and related to the type of soil, on the behavior of t_{grav} . We show that the reformulated t_{grav} (notably $t_{\text{grav}} = F(\beta)S^2/(K_s - K_i)^2$, where $F(\beta)$ is a β -dependent function) is about three times larger than the classical t_{grav} given by $t_{\text{grav,Philip}} = S^2/(K_s - K_i)^2$. The differences between the classical $t_{\text{grav,Philip}}$ and the reformulated t_{grav} increase for fine-textured soils, attributed to the time needed to attain steady-state infiltration and thus $i + n$ infiltration for inferring soil hydraulic properties. Results show that the proposed t_{grav} is a better indicator of time domain validity than $t_{\text{grav,Philip}}$. For the attainment of steady-state infiltration, the reformulated t_{grav} is suitable for coarse-textured soils. Still neither the reformulated t_{grav} nor the classical $t_{\text{grav,Philip}}$ are suitable for fine-textured soils for which t_{grav} is too conservative and $t_{\text{grav,Philip}}$ too short. Using t_{grav} will improve predictions of the soil hydraulic parameters (particularly K_s) from infiltration data compared to $t_{\text{grav,Philip}}$.

1. Introduction

Infiltration is a key hydrological process that partitions precipitation at the land surface into the part that enters the soil profile and the excess water that runs off. Infiltration and runoff trigger various secondary processes including erosion (e.g., Assouline & Ben-Hur, 2006; Garrote & Bras, 1995; Poesen & Valentin, 2003), changes in stream flow and flooding events (e.g., Garrote & Bras, 1995), landslides and debris flows on hillslopes (e.g., Iverson, 2000; Lehmann & Or, 2012), water available for vegetation (e.g., Verhoef & Egea, 2013), as well as groundwater recharge (e.g., Anderson et al., 2015; Villeneuve et al., 2015), while also affecting the exchange of water and energy between soil and the atmosphere (e.g., Kim et al., 2017; MacDonald et al., 2018). Therefore, knowledge about infiltration is of high relevance for various scientific disciplines. A recent comprehensive

© 2022. The Authors.

This is an open access article under the terms of the [Creative Commons Attribution License](https://creativecommons.org/licenses/by/4.0/), which permits use, distribution and reproduction in any medium, provided the original work is properly cited.

Writing – review & editing: Mehdi Rahmati, Borja Latorre, David Moret-Fernández, Laurent Lassabatiere, Nima Talebian, Dane Miller, Renato Morbidelli, Massimo Iovino, Vincenzo Bagarello, Ying Zhao, Jan Vanderborght, Lutz Weihermüller, Rafael Angulo Jaramillo, Dani Or, Martinus Th. van Genuchten, Harry Vereecken

review of Vereecken et al. (2019) highlights the importance of infiltration processes at scales ranging from the pedon to global.

The infiltration process can generally be described by solving the Richards (1931) equation when the relationships between soil water content, matric potential, and hydraulic conductivity are defined explicitly. Alternatively, direct measurement of actual infiltration provides a convenient field approach to determining soil hydraulic parameters such as the sorptivity and saturated hydraulic conductivity (Ross et al., 1996). Sorptivity (S) expresses the capacity of a soil to absorb and release water by capillarity. In contrast, the saturated hydraulic conductivity (K_s) reflects the ability of a soil to transmit water under the influence of gravity.

As a unique solution of the Richards equation, the time series expansion (TSE) introduced by Philip (1957, 1969) remains a widely used model for 1D ponded infiltration. Although, the TSE comprises an infinite series of different components, generally only the first two terms are being used in practice, with the higher-order terms in the infinite time series requiring a more systematic analysis. To analyze the convergence and time domain validity of the TSE, Philip (1969) introduced a characteristic time termed gravity time, t_{grav} , at which gravity begins to dominate infiltration over capillarity. Philip (1969) assumed t_{grav} to be a practical measure for the time range of useful convergence of the TSE to real data, thus allowing use of the two-term TSE. Hereby, t_{grav} was simply formulated in terms of S and $\Delta K = K_s - K_i$, where K_i is the hydraulic conductivity at the initial (prior to infiltration) soil water content, θ_i . Although not mentioned explicitly by Philip (1969), one may infer that only the two first terms of the TSE are used to formulate t_{grav} . The definition of t_{grav} is then explicit since the first term of the infiltration equation represents the effects of capillarity, and the second term the effects of gravity.

The parameter t_{grav} has been used for a range of applications. For example, Ross et al. (1996) used t_{grav} to scale the time and cumulative infiltration to obtain a dimensionless implicit analytical equation for infiltration. In another study on K_s data obtained from positive-head tension and single-ring pressure infiltrometer data with classical undisturbed soil core measurements, Reynolds et al. (2000) used t_{grav} as an index of the time at which steady-state infiltration will be reached. While designing a Beerkan Estimation of Soil Transfer (BEST) method, Lassabatiere et al. (2006) further used t_{grav} to determine the maximum time for which transient expressions should be fitted to experimental data to properly estimate S and K_s . In that case, the authors used the t_{grav} concept to compute the time validity of TSE for other types of analytical models. This last example shows that the concept of t_{grav} developed regarding Philip's TSE may be generalized to other analytical models.

Whether or not t_{grav} is a correct indicator for the time domain validity of Philip's TSE and its truncated forms accuracy, and/or if it is an accurate indicator for attaining steady-state infiltration, a precise determination of t_{grav} itself is still of great importance. A limitation of the two-term infiltration approximation, as used to formulate t_{grav} , is that it cannot be used for long infiltration times. Several studies indicate that the higher-order TSE terms can describe the infiltration process much better the two-term equation for some soils (Kutílek & Krejca, 1987; Rahmati et al., 2019, 2020). On the other hand, conceptually, t_{grav} that marks when 50% of the cumulative infiltration is dominated by capillarity alone offers a generalizable alternative concept that it is valid irrespective of the number of terms included in the infiltration equation as well as regardless of the invoked model. A possible improvement when reformulating t_{grav} could be the use of an infiltration model without any time constraints. An attractive approach for this is the analytic approximation provided by Parlange et al. (1982), further denoted as AAP (Analytic Approximation by Parlange). The analytic approximation of Parlange et al. (1982) has been referred to as a “quasi-exact implicit formulation of Haverkamp et al. (1994) for 1D flow” by several authors. While Haverkamp et al. (1994) introduced useful refinements to the original expression of Parlange et al. (1982), in line with scientific convention, the expression (and modification thereof) should be referred to as the Parlange et al. (1982) equation as suggested by Haverkamp et al. (1994). We will use AAP because this formulation is (a) widely adopted due to its physical basis; (b) valid for the entire infiltration process (Haverkamp et al., 1994; Parlange et al., 1982); and (c) also admits its own TSE by analogy with Philip's TSE (Moret-Fernández et al., 2020; Rahmati et al., 2019, 2020), thus enabling users to determine which component reflects the capillary or gravity effects on infiltration (Rahmati et al., 2020). In addition to S and ΔK , the AAP formulation includes a soil specific shape parameter β that also impacts infiltration and depends on the soil hydraulic parameters. We therefore seek to broaden the formulation of t_{grav} by considering all variables S , $\Delta K = K_s - K_i$, and β as used in the AAP formulation so that the general features of the cumulative infiltration curve can be captured for different soils.

For both the Philip and AAP TSE models, adding terms to the TSE-based t_{grav} formulation reflects the persistent effects of capillarity at relatively long infiltration times when infiltration is dominated by gravity. If the two-term TSE infiltration equation is used, the first term is purely capillary driven and the second term is driven by gravity (Lassabatere et al., 2006; Philip & Farrell, 1964, among others). However, the role of higher-order TSE terms, whether capillary- or gravity-driven, remains controversial, primarily because they contain ratios of K_s^{n-1}/S^{n-2} (with $n = 1, 2, \dots, \infty$). For example, Rahmati et al. (2020, 2021) analyzed the contributions of the higher order TSE terms of the AAP model under the premise that the role of gravity increases with increasing infiltration time. They concluded that although the higher-order terms still include the capillary parameter S , the terms remain largely controlled by gravity. A characteristic of the TSE is that all higher terms (those beyond the first two) have negligible impact on the onset of infiltration, whereas their contribution increases with increasing infiltration time. Since S is a capillary parameter, an important question arises about the role of S in the higher-order TSE terms, and whether these terms mainly reflect gravity. A simple answer to this question can be found in the mathematical form of the infinite series in terms of θ as derived by Philip (1957). The series contains the variables S and K_s for all infiltration times, but with significantly diminishing contributions of S beyond the first (absorption) term. Also, Philip's solution of the Richards (1931) equation involves a perturbation of the exact absorption case without gravity, while also considering uniform soil properties and initial soil water contents. These premises are often violated since the advancing infiltration front may reach layers with different water retention and hydraulic conductivities, thereby physically and mathematically affecting the infiltration rate at the surface. From a physical perspective, gravity will dominate the flow process at late infiltration times, and hence one may expect then vertically downward gravity-driven saturated flow (Waechter & Philip, 1985). However, by neglecting capillarity, no information on the transition from near-dryness to near-saturation in regions below the infiltration front will be obtained. As correctly stated by Waechter and Philip (1985), this is a “physically interesting and practically important limit of flows strongly dominated by gravity, with capillary effects weak but nonzero”.

Because of the above ambiguities in the expression of t_{grav} , this study aims to clarify the definition of the characteristic infiltration time. Specific objectives are to: (a) reformulate the infiltration characteristic time t_{grav} using the AAP formulation of (Parlange et al., 1982), (b) study its relation to the classical t_{grav} introduced by Philip (1969), hereafter denoted as $t_{\text{grav,Philip}}$, and (c) discuss potential applications of this soil property regarding our understanding and modeling of water infiltration into soils.

2. Theoretical Development

2.1. Philip's Infiltration Theory

Based on an exact solution of the Richards (1931) equation, Philip (1957, 1969) derived the following expression for 1D ponded infiltration, known as Philip's TSE:

$$I(t) = A_1 t^{\frac{1}{2}} + (A_2 + K_i) t + \sum_{n=3}^{\infty} A_n t^{\frac{n}{2}} \quad (1)$$

where $I(t)$ denote cumulative infiltration [L] at a given time t [T] and A_1 to A_{∞} [$L/T^{n/2}$] are coefficients of the infinite time series:

$$A_n \geq \frac{K_s^{n-1}}{S^{n-2}}, \quad n = 1, 2, \dots, \infty \quad (2)$$

Philip (1969) showed that A_1 is equal to the sorptivity S , while A_2 is proportional to K_s , suggesting that $A_2 = c(K_s - K_i)$, where c is a constant equal to $1/2$, $2/3$, and 0.38 depending upon the selected diffusivity model (i.e., linearized, a δ -function, and/or nonlinear).

Philip (1969) also determined the time domain validity of his TSE formulation. By comparing time and geometric series expansions, he found that the series solution should converge to the infiltration curve described by the Richard equation for $t < (S/A_2)^2$. By noting that in most cases $K_i/K_s \ll 1$ and $A_2 \approx 1/2(K_s - K_i)$, Philip (1969) concluded that the convergence time or time domain validity could be defined as $t < 4t_{\text{grav, Philip}}$. Using S , K_s , and K_i , he approximated $t_{\text{grav, Philip}}$ as:

$$t_{\text{grav,Philip}} = \left(\frac{S}{K_s - K_i} \right)^2 \quad (3)$$

For initially dry soil conditions such that K_i can be neglected, the above equation simplifies to:

$$t_{\text{grav,Philip}} = \left(\frac{S}{K_s} \right)^2 \quad (4)$$

Philip (1969) furthermore showed that the condition $t < 4t_{\text{grav,Philip}}$ was too conservative and that the factor 4 could be replaced by a smaller value. He then stated that, nominally, $t \leq t_{\text{grav,Philip}}$ expresses the practical time domain validity for the TSE. We note that prior to Philip (1969), Philip and Farrell (1964) had defined the infiltration characteristic time, $t_{\text{grav,P\&F}}$, as well as the infiltration characteristic length, $I_{\text{grav,P\&F}}$, as:

$$t_{\text{grav,P\&F}} = \left(\frac{S}{c(K_s - K_i)} \right)^2 \xrightarrow{K_i \approx 0} t_{\text{grav,P\&F}} = \left(\frac{S}{cK_s} \right)^2 \quad (5a)$$

$$I_{\text{grav,P\&F}} = \frac{S^2}{c(K_s - K_i)} \xrightarrow{K_i \approx 0} I_{\text{grav,P\&F}} = \frac{S^2}{cK_s} \quad (5b)$$

2.2. Parlange's Analytical Solution of the Infiltration Equation

Equation 3 holds subject to the approximate time constraint that an attractive approach to overcome the time constraint is through comparisons with AAP. The AAP solution, which is valid for all times and gives an accurate estimate of the cumulative infiltration, can also be expanded in two-term (2T), three-term (3T) or higher approximations, via the same approach of TSEs (e.g., Lassabatere et al., 2009). These models may be used to provide a more reliable estimate of t_{grav} . We first provide a background of the AAP as summarized by Rahmati et al. (2020).

The AAP cumulative infiltration solution (Parlange et al., 1982), which was redefined by Haverkamp et al. (1994), is given by:

$$\frac{2\Delta K^2}{S^2}t = \frac{2}{1-\beta} \frac{\Delta K(I - K_i t)}{S^2} - \frac{1}{1-\beta} \ln \left[\frac{1}{\beta} \exp \left\{ \frac{2\beta \Delta K(I - K_i t)}{S^2} \right\} + \frac{\beta - 1}{\beta} \right] \quad (6)$$

where β is a soil-dependent dimensionless integral shape parameter, usually fixed at 0.6 (default value). Fuentes et al. (1992) demonstrated that the shape parameter β is related to the soil hydraulic functions by:

$$\beta = 2 - 2 \frac{\int_{\theta_i}^{\theta_s} \left(\frac{K - K_i}{K_s - K_i} \right) \left(\frac{\theta_s - \theta_i}{\theta - \theta_i} \right) D(\theta) d\theta}{\int_{\theta_i}^{\theta_s} D(\theta) d\theta} \quad (7)$$

where θ_s is the saturated volumetric water content (L^3L^{-3}), θ_i is the initial water content (L^3L^{-3}), and $D(\theta)$ is the soil water diffusivity. For initially dry soils (with $K_i \sim 0$), the AAP solution reduces to:

$$\frac{2K_s^2}{S^2}t = \frac{2}{1-\beta} \frac{K_s I}{S^2} - \frac{1}{1-\beta} \ln \left[\frac{1}{\beta} \exp \left(\frac{2\beta K_s I}{S^2} \right) + \frac{\beta - 1}{\beta} \right] \quad (8)$$

A simplified two-term (2T) approximate expansion of Equation 8 was proposed by Haverkamp et al. (1994) to describe the transient state valid for short to intermediate infiltration times. The expansion is identical to Philip (1957) two-term equation:

$$I(t) = c(1)t^{\frac{1}{2}} + c(2)t \quad (9)$$

where

$$\begin{aligned} c(1) &= S \\ c(2) &= \frac{2-\beta}{3} K_s \end{aligned} \quad (10)$$

Additional expansions were proposed by Rahmati et al. (2019) using three terms (3T), by Moret-Fernández et al. (2020) considering four terms (4T), and Rahmati et al. (2020) using five terms (5T), that is,

$$I(t) = c(1)t^{\frac{1}{2}} + c(2)t + c(3)t^{\frac{3}{2}} \quad (11)$$

$$I(t) = c(1)t^{\frac{1}{2}} + c(2)t + c(3)t^{\frac{3}{2}} + c(4)t^2 \quad (12)$$

$$I(t) = c(1)t^{\frac{1}{2}} + c(2)t + c(3)t^{\frac{3}{2}} + c(4)t^2 + c(5)t^{\frac{5}{2}} \quad (13)$$

where $c(3)$ to $c(5)$ are defined as:

$$\begin{aligned} c(3) &= \frac{1}{9} (\beta^2 - \beta + 1) \frac{K_s^2}{S} \\ c(4) &= \frac{2}{135} (\beta - 2)(\beta + 1)(1 - 2\beta) \frac{K_s^3}{S^2} \\ c(5) &= \frac{1}{270} (\beta^2 - \beta + 1)^2 \frac{K_s^4}{S^3} \end{aligned} \quad (14)$$

These expressions for $c(3)$ to $c(5)$ assume that the initial hydraulic conductivity is negligible. We adopt this hypothesis to simplify the derivations of t_{grav} . We aim at simplifying t_{grav} by (a) neglecting the initial hydraulic conductivity and thus neglecting the dependency of t_{grav} on initial conditions and (b) using the approximate expansions instead of the implicit AAP model to ease computations.

2.3. Exact Implicit Formulation of the Characteristic Time t_{grav}

According to the basic definition of t_{grav} , one can rewrite any TSE at time equal to t_{grav} as (Rahmati et al., 2020):

$$\frac{1}{2} I_{\text{grav}} = S t_{\text{grav}}^{\frac{1}{2}} \quad (15)$$

where I_{grav} is the cumulative infiltration at time t_{grav} , also known as the infiltration characteristic length. I_{grav} in Equation 15 can be computed immediately by evaluating any analytical model at time t_{grav} . Since Philip's TSE is not clearly defined when using a limited number of terms, we consider it more robust to reformulate t_{grav} by using the AAP solution, which is valid for all infiltration times. To do this, Equation 6 is redefined in terms of $t = t_{\text{grav}}$ by substituting I_{grav} from Equation 15 into Equation 6 to give:

$$\frac{2\Delta K^2}{S^2} t_{\text{grav}} = \frac{2}{1-\beta} \frac{\Delta K \left(2S t_{\text{grav}}^{\frac{1}{2}} - K_i t_{\text{grav}} \right)}{S^2} - \frac{1}{1-\beta} \ln \left[\frac{1}{\beta} \exp \left\{ \frac{2\beta \Delta K \left(2S t_{\text{grav}}^{\frac{1}{2}} - K_i t_{\text{grav}} \right)}{S^2} \right\} + \frac{\beta - 1}{\beta} \right] \quad (16)$$

If K_s , K_i , $\Delta K (=K_s - K_i)$, S , and β are known, this equation can be solved analytically for t_{grav} using MATLAB, Mathematica, R, Python, or some other appropriate software. Those approaches can be combined with scaling procedures to separate the effects of scale and the hydraulic shape parameters. A computationally more effective scaling procedure as proposed by Varado et al. (2006) and further developed by Lassabatere et al. (2009), also for the sorptivity (Lassabatere et al., 2021) can be used. For this purpose, we scale cumulative infiltration, $I(t)$, and time, t , by:

$$I(t) = \frac{S^2}{2\Delta K} I^*(t^*) + K_i t \quad (17a)$$

$$t = \frac{S^2}{2\Delta K^2} t^* \quad (17b)$$

Rewriting the above equations for $t = t_{\text{grav}}$ yields:

$$\begin{aligned} I(t_{\text{grav}}) &= \frac{S^2}{2\Delta K} I^*(t_{\text{grav}}^*) + \frac{S^2 K_i}{2\Delta K^2} t_{\text{grav}}^* \\ t_{\text{grav}} &= \frac{S^2}{2\Delta K^2} t_{\text{grav}}^* \end{aligned} \quad (18)$$

where t_{grav}^* is the scaled t_{grav} parameter, and $I^*(t_{\text{grav}}^*)$ corresponds to the scaled cumulative infiltration at t_{grav}^* . Substitution of the above expressions into Equation 16 leads to:

$$t_{\text{grav}}^* = \frac{1}{1-\beta} \left(2\sqrt{2t_{\text{grav}}^*} - \frac{K_i}{\Delta K} t_{\text{grav}}^* \right) - \frac{1}{1-\beta} \ln \left[\frac{1}{\beta} \exp \left\{ \beta \left(2\sqrt{2t_{\text{grav}}^*} - \frac{K_i}{\Delta K} t_{\text{grav}}^* \right) \right\} + \frac{\beta-1}{\beta} \right] \quad (19)$$

Several functions for the hydraulic conductivity could be used in Equation 19. For this study we used the Mualem–van Genuchten (MvG) model (Mualem, 1976; van Genuchten, 1980) for K_i given by:

$$\frac{K(S_e)}{K_s} = S_e^{1/2} \left[1 - \left(1 - S_e^{1/m} \right)^m \right]^2, \quad S_e = \frac{\theta - \theta_r}{\theta_s - \theta_r} \quad (20)$$

where $K(S_e)$ is soil hydraulic conductivity at effective saturation (S_e), or alternatively at a given soil water content θ , m is a model parameter, and θ_s and θ_r are the saturated and residual water contents ($\text{L}^3 \text{L}^{-3}$), respectively. Substitution of Equation 20 into Equation 19 gives:

$$t_{\text{grav}}^* = \frac{1}{1-\beta} \left(2\sqrt{2t_{\text{grav}}^*} - \delta t_{\text{grav}}^* \right) - \frac{1}{1-\beta} \ln \left[\frac{1}{\beta} \exp \left\{ \beta \left(2\sqrt{2t_{\text{grav}}^*} - \delta t_{\text{grav}}^* \right) \right\} + \frac{\beta-1}{\beta} \right] \quad (21)$$

where δ is a coefficient accounting for the effects of initial soil water content and the parameter m on t_{grav}^* :

$$\delta = \frac{S_{e,i}^{1/2} \left[1 - \left(1 - S_{e,i}^{1/m} \right)^m \right]^2}{1 - S_{e,i}^{1/2} \left[1 - \left(1 - S_{e,i}^{1/m} \right)^m \right]^2}, \quad 0 \leq \delta < 1 \quad (22)$$

Equation 21 is identical to Equation 16, except that K_s , K_i , and S are eliminated to lead to a more generalized dimensionless definition of t_{grav}^* from where we can view t_{grav}^* as a function of the infiltration-related soil variable β and the functional coefficient δ given by:

$$t_{\text{grav}}^* = c(\beta, \delta) \quad (23)$$

The function $c(\beta, \delta)$ is to be obtained from Equation 21 by numerical resolution using a root-finding algorithm. Finally, the dimensional t_{grav} can be recovered immediately from Equation 17b to yield:

$$t_{\text{grav}} = F(\beta, \delta) \left(\frac{S}{\Delta K} \right)^2 \quad (24)$$

where $F(\beta, \delta)$ defines a functional relationship depending on β and δ :

$$F(\beta, \delta) = \frac{c(\beta, \delta)}{2} \quad (25)$$

For an initially dry soil ($\lim_{S_{e,i} \rightarrow 0} \delta = 0$), one can simply set $\delta = 0$. Equation 21 then simplifies to:

$$t_{\text{grav}}^* = \frac{1}{1-\beta} \left(2\sqrt{2t_{\text{grav}}^*} - \ln \left[\frac{1}{\beta} \exp \left\{ 2\beta \sqrt{2t_{\text{grav}}^*} \right\} + \frac{\beta-1}{\beta} \right] \right) \quad (26)$$

In this case, t_{grav}^* may be viewed as a function of β only. Equation 24 can then be simplified also by setting $K_i = 0$:

$$t_{\text{grav}} = F(\beta, \delta = 0) \left(\frac{S}{K_s} \right)^2 = F(\beta) \left(\frac{S}{K_s} \right)^2 \quad (27)$$

By having t_{grav} reformulated, one can simply use Equation 15 to compute the infiltration characteristic length by:

$$I_{grav} = 2\sqrt{F(\beta, \delta)} \frac{S^2}{\Delta K} \xrightarrow{K_i \approx 0} I_{grav} = 2\sqrt{F(\beta)} \frac{S^2}{K_s} \quad (28)$$

2.4. An Approximate Explicit Expression of the Characteristic Time t_{grav}

Although formally it is possible to evaluate the functional relationship $F(\beta)$ numerically, the equation might be too impractical for many applications. Therefore, we use the 3T approximation (i.e., 3T TSE of the AAP model) alternatively to obtain an explicit formulation for $F(\beta)$ and consequently for t_{grav} . Calculating I_{grav} at time t_{grav} using the 3T approximation (Equation 11), and substituting it in Equation 15, yields:

$$S = \frac{1}{2} \frac{St_{grav}^{\frac{1}{2}} + \frac{2-\beta}{3} K_s t_{grav} + \frac{1}{9} (\beta^2 - \beta + 1) \frac{K_s^2}{S} t_{grav}^{\frac{3}{2}}}{t_{grav}^{\frac{1}{2}}} \quad (29)$$

In this expression, the initial value of the hydraulic conductivity, K_i , is neglected, meaning that the expression should be considered only for initially dry soils. Simplifying and rearranging Equation 29 results in a quadratic equation, where $\sqrt{t_{grav}}$ represents an unknown, and K_s , S , and β are knowns:

$$-S + \frac{2-\beta}{3} K_s t_{grav}^{\frac{1}{2}} + \frac{1}{9} (\beta^2 - \beta + 1) \frac{K_s^2}{S} t_{grav} = 0 \quad (30)$$

Solving Equation 30 for $\sqrt{t_{grav}}$ in terms of its positive root results in the following expression:

$$F(\beta) = \left(\frac{3}{2} \frac{\sqrt{5\beta^2 - 8\beta + 8} - (2 - \beta)}{(\beta^2 - \beta + 1)} \right)^2 \quad (31)$$

which shows that $F(\beta)$ now explicitly depends on β .

2.5. Test Data for Validation

The expressions above were obtained by using the AAP expansion. However, when evaluating their AAP based model, Parlange et al. (1982) made several assumptions that may not apply to real-world cases, such as the choice of the $\theta(z, t)$ profile as well as interpolation of the relationship between diffusivity and hydraulic conductivity. Their proposed relation between β and the soil hydraulic curves (see Equation 6 in Haverkamp et al., 1994) seems problematic and not applicable at all times. This point was discussed in-depth by Lassabatere et al. (2009), who showed that the relation holds poorly for some types of soils (see Figure 6 of Lassabatere et al., 2009). Apart from the AAP limitations, using infiltration data simulated with HYDRUS to validate t_{grav} is more scientifically sound. For this reason, we validated the proposed expressions of $F(\beta, \delta)$ against synthetic infiltration data generated with the HYDRUS-1D software (Šimůnek et al., 2008, 2016). For the HYDRUS simulations we used the soil hydraulic properties of the 12 USDA soil textural classes (Table 1) provided by Carsel and Parrish (1988). Table 2 summarizes the settings of the HYDRUS simulations.

The numerically generated data are considered as the reference data and used in the following to assess the accuracy of the approximate expansions, including those related to Philip's and the AAP TSE formulations.

2.6. Time Domain Validity and Time to Steady-State Infiltration

For this section we considered the scenarios detailed in Table 1, which were modeled with HYDRUS to obtain reference cumulative infiltration data. We then computed the Philip and AAP TSE expansions from the previously computed input parameters S , K_s , K_i , and β . Note that β was computed using Fuentes' equation (Equation 7). The initial hydraulic conductivity was computed using Equation 20. Lastly, sorptivity (S) data were obtained from horizontal infiltration simulations by Rahmati et al. (2020). The Philip and AAP TSE predictions were compared to the numerically generated data described in the previous section by considering pointwise differences between predicted $\hat{I}(t)$ and numerically simulated $I(t)$ values:

Table 1

Soil Hydraulic Parameters of the Mualem-van Genuchten (MvG) Model (van Genuchten (1980) for the Soil Water Retention and Hydraulic Conductivity Functions for the 12 USDA Textural Classes According to Carsel and Parrish (1988)

Parameters	θ_r	θ_s	θ_i	α	n (-)	m (-)	K_s	S	β (-)
	(cm ³ cm ⁻³)			(cm ⁻¹)			(cm h ^{-1/2})	(cm h ^{-1/2})	
Clay	0.068	0.380	0.271	0.008	1.09	0.083	0.20	1.02	1.92
Clay loam	0.095	0.410	0.150	0.019	1.31	0.237	0.26	1.46	1.58
Loam	0.078	0.430	0.088	0.036	1.56	0.359	1.04	2.20	1.27
Loamy sand	0.057	0.410	0.057	0.124	2.28	0.561	14.6	6.22	0.80
Sand	0.045	0.430	0.045	0.145	2.68	0.627	29.7	9.23	0.60
Sandy clay	0.100	0.380	0.170	0.027	1.23	0.187	0.12	0.79	1.70
Sandy clay loam	0.100	0.390	0.111	0.059	1.48	0.324	1.31	1.61	1.36
Sandy loam	0.065	0.410	0.066	0.075	1.89	0.471	4.42	3.84	0.99
Silt	0.034	0.460	0.090	0.016	1.37	0.270	0.25	1.35	1.50
Silt loam	0.067	0.450	0.104	0.020	1.41	0.291	0.45	1.66	1.44
Silt clay	0.070	0.360	0.266	0.005	1.09	0.083	0.02	0.35	1.92
Silty clay loam	0.089	0.430	0.197	0.010	1.23	0.187	0.07	0.53	1.70

Note. The sorptivity (S) data were obtained from horizontal infiltration simulations by Rahmati et al. (2020). The tortuosity parameter l for the hydraulic conductivity was fixed at 0.5 as used by van Genuchten (1980). Initial water contents θ_i at an initial pressure head of $-10,000$ cm were taken from Rahmati et al. (2020, 2021). The infiltration constant β was calculated using Equation 7. θ_s , θ_r , and θ_i are the saturated, residual, and initial water contents; α , n , and m are parameters of the van Genuchten (1980) soil hydraulic model; K_s is the saturated hydraulic conductivity; S is the soil sorptivity; β is an infiltration constant defined by Parlange et al. (1982) and formulated by Fuentes et al. (1992).

$$d(t) = \frac{|\hat{I}(t) - I(t)|}{I(t)} \times 100 \quad (32)$$

where d is the distance/difference between the targeted approximate expansion and numerically simulated infiltration per each unit cumulative infiltration at a certain time step t . Theoretically, when the time domain validity of the approximate expansions is targeted, $d(t)$ will have lower values at initial times, but then will tend toward higher values at later times. Practically, the time where $d(t)$ exceeds a critical value, $d(t) \geq d_{TDV}$, is considered as the time beyond which the approximate expansion is not valid anymore. For this analysis we used a d_{TDV} threshold of 5%.

Table 2

Parameters and Conditions Used for the HYDRUS-1D Simulations to Generate the Synthetic Infiltration Data (Adopted From Rahmati et al., 2020, 2021)

Simulation settings	Applied conditions
Soil Profile depth	200 cm
Upper boundary condition	Zero-pressure head
Lower boundary condition	Free drainage
Node Numbers for discretization	401 non-equidistant (finer spacing near the top)
Simulation time	24 hr
Internal interpolation tables	Disabled
Hydraulic model	
if $n > 1.2$	MvG
if $n < 1.2$	Modified MvG with an air-entry value of -2 cm

Note. n is a parameter in the Mualem-van Genuchten (MvG) soil hydraulic functions (van Genuchten (1980)).

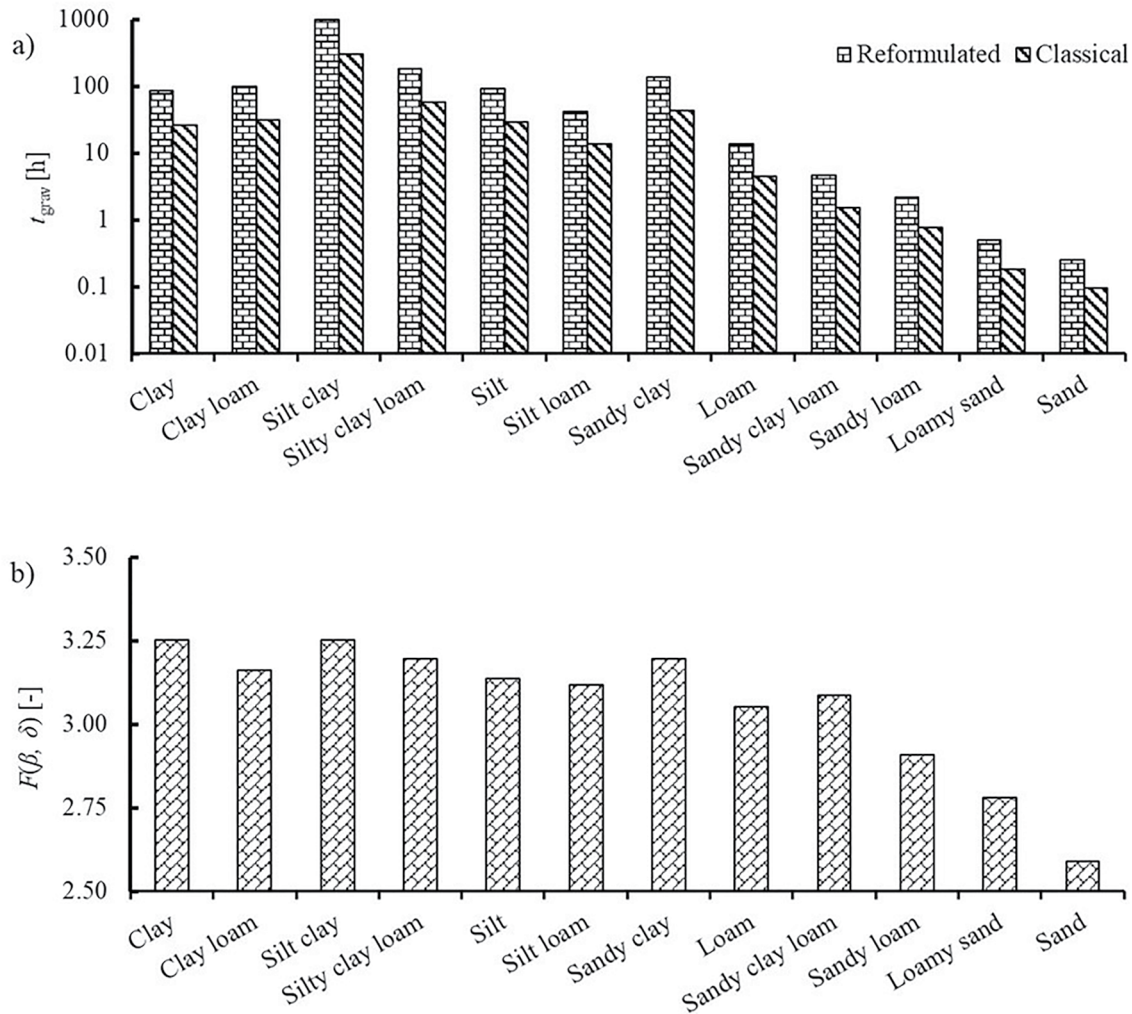


Figure 1. Variations in (a) the reformulated and classical characteristic times (t_{grav} [h]) and (b) the functional relationship $F(\beta, \delta)$ for the 12 USDA soil textural classes. Note that soils are ranked based on their texture and no function is defined for them.

To determine the attainment of the steady-state infiltration, we simply computed a linear regression of the last points and verified that the slope is equal to K_s . Then, having predicted the steady-state infiltration, the time where the numerically simulated HYDRUS-1D cumulative infiltration curve starts to converge to the steady-state line determines the attainment of steady-state infiltration. The same criterion as introduced in Equation 32 has been used to find the time for the attainment of the steady-state infiltration. Theoretically, if the steady-state attainment is reached, $d(t)$ will be higher at short times and tend toward zero with progressing in time. Practically, the time when $d(t)$ drops below a critical value, $d(t) \leq d_{SSI}$, is considered as the time for attaining steady-state infiltration. A d_{SSI} threshold of 5% was used for all soils in this analysis.

3. Results and Discussion

3.1. Functional Relationships for $F(\beta, \delta)$ and t_{grav}

Figure 1 illustrates variations in the functional $F(\beta, \delta)$ given by Equation 25, t_{grav} (i.e., the reformulated t_{grav} obtained for the AAP solution when δ is not set to zero) and $t_{grav, Philip}$ for the 12 USDA soil classes examined. Note that the values of $F(\beta, \delta)$ correspond to the roots of Equation 21, with the values of β tabulated in Table 1 and the values of δ defined by Equation 22. t_{grav} is then directly obtained by scaling time with Equation 24. Figure 2 illustrates the employed δ values to obtain Figure 1.

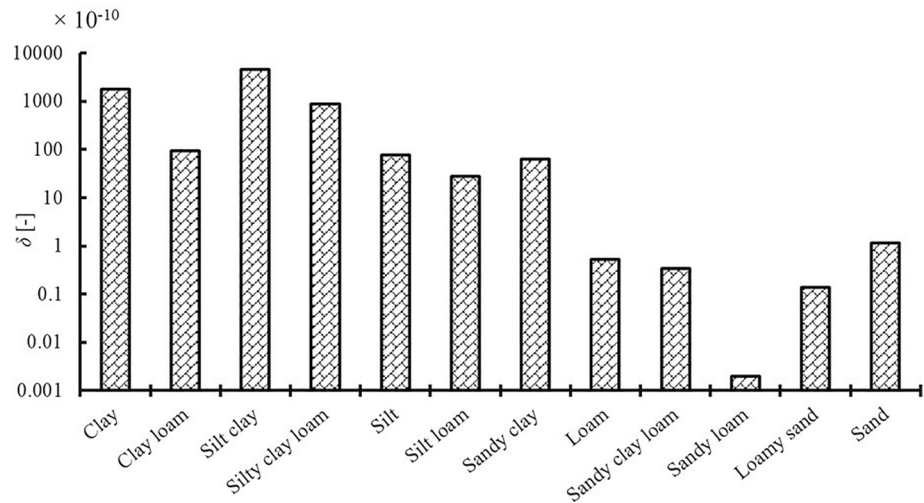


Figure 2. Variation in the functional coefficient δ among the 12 USDA soil textural classes. The δ values were obtained for initial water contents θ_i provided in Table 1.

The results indicate that t_{grav} varies between 15 min for sand and 996 hr for silty clay, with an average of 138 ± 80 hr and a median of 64 ± 60 hr over all soil classes. Excluding silty clay from the analysis, the range of t_{grav} gets narrower by varying between 15 min for sand and 183 hr for silty clay loam, with an average of 60 ± 19 hr and a median of 42 ± 42 hr. The reason why the silty clay soil is an outlier is still unresolved. One reason may be that the MvG parameters were taken from the class pedo-transfer function of Carsel and Parrish (1988). A clear trend can be detected in that the coarser textures have lower t_{grav} values. This agrees with the physics of the flow processes involved, in that lower soil capillary forces and higher flow rates are to be expected for the more coarse-textured soils with their larger pores.

Similarly to t_{grav} , Figure 1 shows that $F(\beta, \delta)$ varies between 2.59 and 3.25, with the finer soil textural classes exhibiting higher $F(\beta, \delta)$ values. These results indicate that the reformulated t_{grav} is approximately 2.59–3.25 times (with a mean value of 3.1) higher than $t_{\text{grav,Philip}}$, since $t_{\text{grav}} = F(\beta, \delta) \times t_{\text{grav,Philip}}$. This probably also impacts the interpretation of infiltration data presented later in Section 3.5. If we consider the relationship between $t_{\text{grav,P\&F}}$ and $t_{\text{grav,Philip}}$ (i.e., $t_{\text{grav,P\&F}} = (1/c)^2 \times t_{\text{grav,Philip}}$) and use the possible range for c parameter (1/3, 2/3) as reported by Philip (1969), $t_{\text{grav,P\&F}}$ will be almost 2.3–9 times the value of $t_{\text{grav,Philip}}$. Therefore, we believe that our reformulated t_{grav} nicely defines this characteristic time by falling between those defined by Philip (1969) and Philip and Farrell (1964).

Next, the relationships between $F(\beta, \delta)$ versus β and δ were analyzed. As can be seen from the contour plot in Figure 3, $F(\beta, \delta)$ is mainly controlled by, and positively correlated to, β throughout most δ values. Additionally, we found that at increasing values of δ , $F(\beta, \delta)$ is dominated by δ . The threshold, where δ dominates the function ranges from around $\delta = 0.1$ in coarse-textured soils with lower β values, to around 0.005 in fine-textured soils with higher β values. However, closer inspection reveals that we rarely find situations in nature where δ exceeds these threshold values where a δ value of 1 corresponds to K_i/K_s of 0.5. An in-depth discussion considering the dependency of δ on m and $S_{e,i}$ is provided in the following section.

3.2. $F(\beta, \delta)$ Versus $F(\beta)$

The effect of δ on t_{grav} was explored by comparing $F(\beta, \delta)$ and $F(\beta)$, where $F(\beta)$ is equal to $F(\beta, \delta)$ when δ is set to zero, that is, $F(\beta) = F(\beta, \delta = 0)$. Our analysis in the previous section showed that δ has a minimal influence on $F(\beta, \delta)$ and that setting $\delta = 0$ did not lead to considerable changes in the $F(\beta, \delta)$ values, and consequently also not in t_{grav} . Our numerical calculations also showed that by setting $\delta = 0$, one will obtain the same results for both cases as shown in Figure 1, which may be a consequence of the δ values being very close to zero for all examined soil classes, except for clay and silty clay, and to a lesser extent also for silty clay loam (Figure 2).

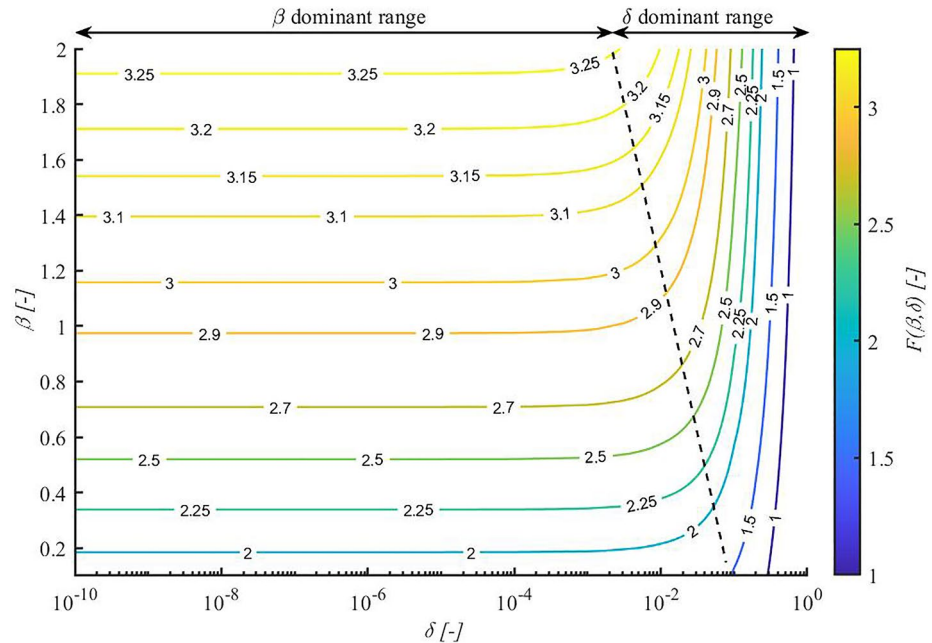


Figure 3. Functional relationship of $F(\beta, \delta)$ within logical ranges of β (0-2) and δ (0-1).

For a more detailed examination of the effect of δ on $F(\beta, \delta)$, and consequently on t_{grav} , the surface response function between $F(\beta, \delta)$, m , and $S_{e,i}$ was explored (Figure 4), whereby all parameters were allowed to vary within a physically meaningful range. To do this, β values must be determined from the m parameter since there is logical relationship between both parameters. In this sense, an empirical linear function of $\beta(m) = 2.141 - 2.421 \times m$ with R^2 value of 0.999 was used to determine β for different m values based on the β and m values tabulated in Table 1 for the different soils. The m values were allowed to vary between 0 and 0.7, the latter corresponding to the highest n value (here $m = 1 - 1/n$) among the studied soil classes. Note that smaller m values generally correspond to more fine-textured soils, while higher m values correspond to coarser-textured ones. We varied $S_{e,i}$ between 0 and 0.9 since $S_{e,i}$ values above 0.9, which correspond to near saturation, may lead to lower infiltration rates. As can be seen from Figure 4, the contour lines are horizontally aligned for the case $m < 0.4$ (medium- and fine-textured soils) and $S_{e,i}$ values less than 0.6, indicating that $S_{e,i}$ starts to affect $F(\beta, \delta)$ only when the soils are close to saturation. The horizontal contour lines can be found for all soils with any possible m value as long as $S_{e,i}$ is lower than 0.5. Figure 4 therefore clearly indicates that $S_{e,i}$, and consequently δ , have considerable effect on $F(\beta, \delta)$ and t_{grav} only when infiltration occurs in coarse-textured soils at a relatively high degree of saturation (e.g., $S_{e,i} > 0.6$) at the start of the infiltration process. The latter condition seldom occurs in nature since coarse-textured soils usually are drained fast after saturation. On the other hand, the possible effects of the m parameter on $F(\beta, \delta)$ and t_{grav} is well explained by the β parameter due to their interlinked relationship. Hence, we are confident that ignoring δ in our formulation will not impact the overall predictions. Consequently, we use $F(\beta, \delta = 0)$ whenever the AAP solution for t_{grav} is used, while for simplicity we use only the term $F(\beta)$ throughout the text.

3.3. Implicit Versus Explicit Solutions of t_{grav}

Still needed is a verification that the much simpler explicit solutions given by Equation 31 provide accurate approximations of the implicit solutions of t_{grav} as given by Equation 21. Figure 5 shows variations in $F(\beta)$ versus β for the 12 soil textural classes when using AAP and the related 3, 4, and 5T expansions. In case of the implicit solution of t_{grav} , $F(\beta)$ was always higher than 2.6 for all textural classes, with $F(\beta)$ linearly increasing with increasing β (Figure 5, AAP). In contrast, a second-order polynomial trend between $F(\beta)$ and β is present when the 3T explicit solution is used, with a maximum of about 3.6 in $F(\beta)$ when β values were about 1.3, and lower $F(\beta)$ elsewhere. A similar trend as for the implicit solution of t_{grav} albeit with a smaller slope, existed between $F(\beta)$

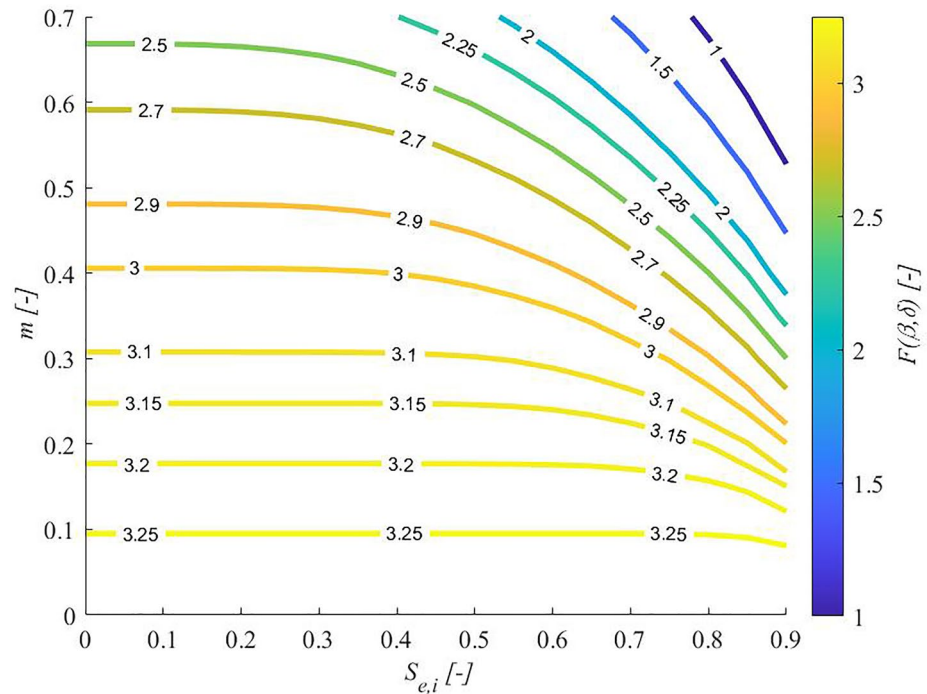


Figure 4. Functional relationship $F(\beta, \delta)$ within logical ranges of the initial saturation degree of soils, $S_{e,i}$, (0–1), and the m parameter (0–0.7). To plot this figure, an empirical function was considered between β and m (i.e., $\beta(m) = 2.141 - 2.421 m$ as derived from the values in Table 1), while δ was determined as a function of m and $S_{e,i}$ using Equation 22.

and β when the 4T expansion was used. The 5 T approximate expansion also showed a second-order polynomial trend between $F(\beta)$ and β , but less nonlinear and with mostly a negative slope.

Figure 5 indicates that the approximate expansions are relatively far away from the implicit solution of t_{grav} , especially at long infiltration times, with the $F(\beta)$ values showing that the reformulated equation for t_{grav} is 2.69–3.25 times larger than the classical t_{grav} model given by Equation 3. These results indicate that precise calculations of t_{grav} requires Parlange's AAP solution instead of the AAP approximate expansions. We explored this more directly by comparing the obtained t_{grav} values from the implicit and explicit solutions, Equation 31. Figure 6 shows the expected differences in t_{grav} between the implicit and explicit solutions. We excluded the 4 and 5T expansions since they are complicated to solve and still inaccurate compared to the AAP implicit solution (especially for large β values). To check the null hypothesis that the pairwise difference between the t_{grav} vectors has a mean equal to zero, a paired-sample t -test at a probability of $p < 0.05$ was performed. The t_{grav} values obtained from the

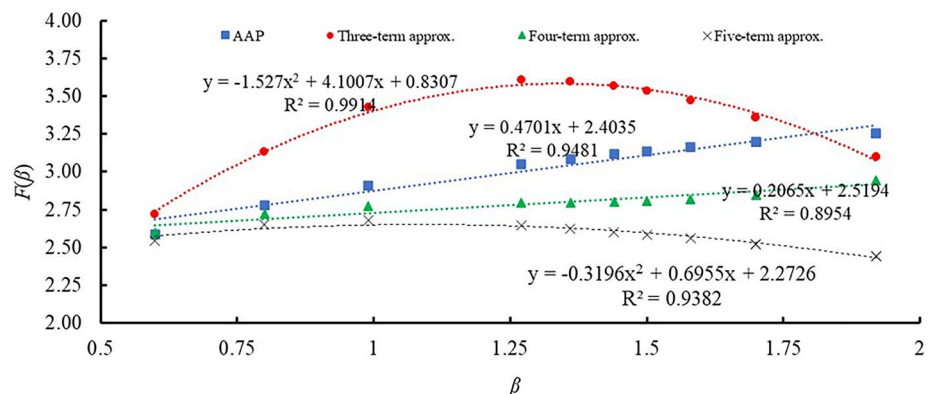


Figure 5. Variations in the function $F(\beta)$ versus β for the 12 USDA soil textural classes, as a function of the selected formulation: AAP, and related 3, 4, or 5T approximate expansions.

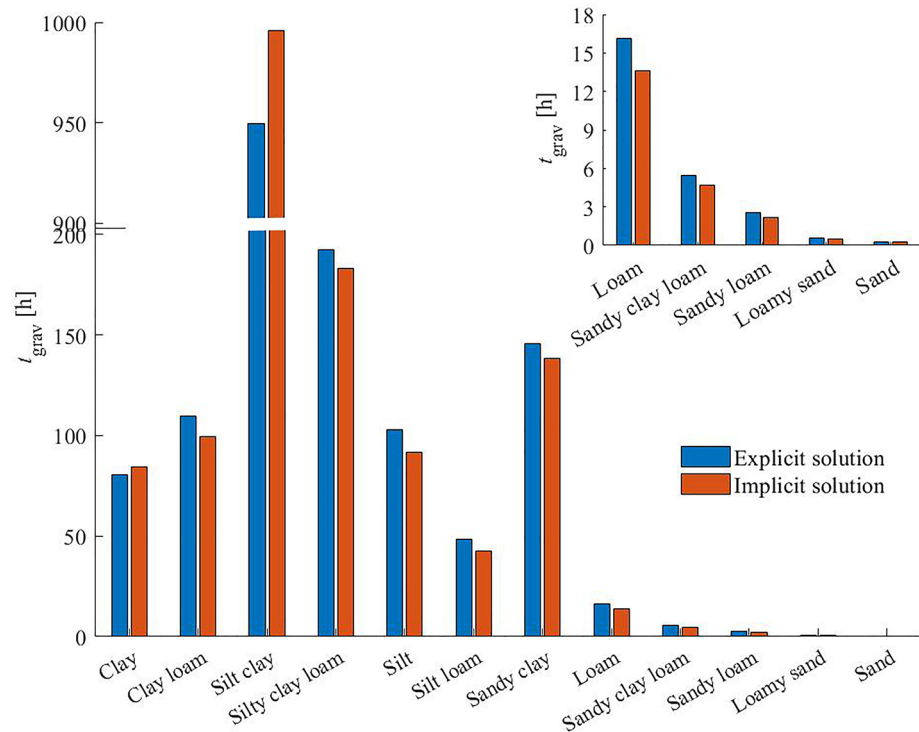


Figure 6. Variations in the soil characteristic time, t_{grav} , determined using the implicit and explicit solutions (based on three terms) of t_{grav} for the examined soil textural classes. The inset shows differences between the two approaches for the coarser soils. Note that the ordinate is split for better visualization.

implicit solution was considered to be the reference value (\hat{t}_{grav}) for comparisons. The results (Table 3) indicate that the differences in the t_{grav} values obtained from the implicit and explicit solutions are significant. As shown in Figure 7, for some soils, the relative difference, $(t_{grav} - \hat{t}_{grav}) / \hat{t}_{grav} \times 100$, is relatively high. For example, for the loam soil, the difference reached almost 18% (Figure 7). Overall, the relative difference was soil type-dependent, with the fine- and coarse-textured soils showing lower ($\pm 5\%$) differences, while for the medium-textured soils the

t_{grav} explicit solution was overestimated by 10%–18%. Therefore, we recommend using the implicit solution for future use. Still, using this solution is very time-consuming and complicated since it requires a numerical solution to estimate t_{grav} using the AAP formulation. Therefore, we suggest applying the following empirical expression between $F(\beta)$ and β , which is obtained for the implicit solution from the data shown in Figure 5:

$$F(\beta) = 0.470\beta + 2.404 \quad (33)$$

Using this empirical expression, $F(\beta)$ can be obtained for β values between 0.6 and 2.

3.4. Influence of β on t_{grav}

Given the fact that β is very difficult to estimate and its value has little effect on 1D cumulative infiltration rates (e.g., Latorre et al., 2018; Rahmati et al., 2020), we analyzed the effect of β on t_{grav} using a constant values of 0.6 for β of 0.6 as suggested by Haverkamp et al. (1994), rather than a soil-dependent β according to Equation 7, for both the implicit and explicit solutions. As can be seen from Figure 8, a constant β value of 0.6 does not represent t_{grav} very well for none of the USDA soil classes (except for sand

Table 3
Results of the Paired-Sample t -Test Between t_{grav} Values Obtained From Implicit and Explicit Solutions

	Implicit	Explicit
Mean ^a	1.347	1.383
Variance	1.221	1.187
Observations	12	12
Pearson Correlation	0.9997	
Hypothesized Mean Difference	0	
Degree of Freedom, df	11	
t -stat	−3.868	
$P(T \leq t)$ one-tail	1.31E−03	
t -Critical, one-tail	1.796	
$P(T \leq t)$, two-tail	2.62E−03	
t -Critical, two-tail	2.201	

^aLogarithms (\log_{10}) of t_{grav} data were used in the analysis to ensure a normal distribution of the data.

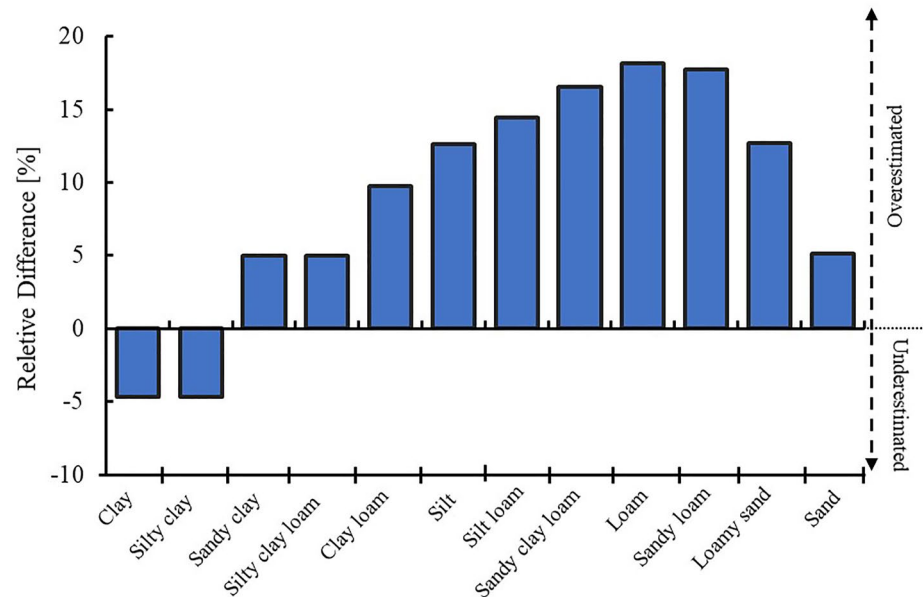


Figure 7. Relative differences, $(t_{grav} - \hat{t}_{grav}) / \hat{t}_{grav} \times 100$, between characteristic times determined using the implicit (\hat{t}_{grav}) and explicit (t_{grav}) solutions (based on three terms) for the examined soil textural classes.

which originally had a β value of 0.6), neither when the implicit nor explicit solution was used. In both cases, using a constant β value resulted in up to 25% underestimations in the t_{grav} predictions. The course the soil texture, the less the underestimation was caused by a constant β value. In other words, the finer the soil texture, the higher the deviation of t_{grav} values obtained when constant and soil-dependent β values were used. The reason is that fine-textured soils usually have β values almost double or even larger than the constant value of 0.6.

To compare the soil-dependent and constant β cases when the implicit or explicit solution is used, a paired-sample t -test at $p < 0.05$ showed (Table 4) that our null hypothesis that the pairwise difference between the t_{grav} vectors

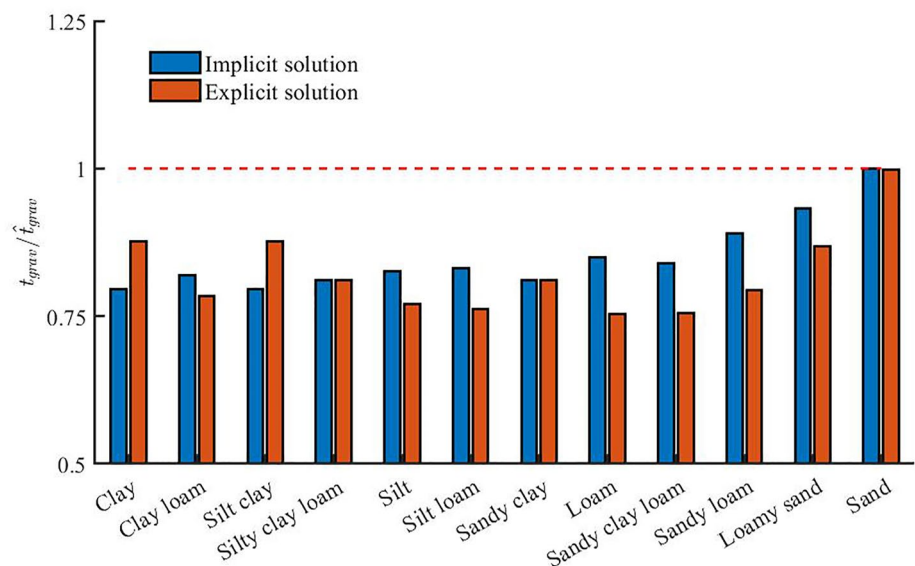


Figure 8. The ratios between soil characteristic times, t_{grav} , determined by implicit or explicit solutions when soil-dependent β values (Equation 7) and constant β value of 0.6 (Haverkamp et al., 1994) are applied. In both solutions, t_{grav} values obtained from soil-dependent β values are considered as reference (\hat{t}_{grav}) for comparisons.

Table 4

Results of the Paired-Sample t -Test Between t_{grav} Values Obtained With the Implicit and Explicit Solutions Along With Soil-Dependent β Values (Equation 7) and a Constant Value of 0.6 as Suggested by Haverkamp et al. (1994)

	Implicit solution		Explicit solution	
	Soil-dependent β	Constant β	Soil-dependent β	Constant β
Mean ^a	1.347	1.275	1.383	1.297
Variance	1.221	1.160	1.187	1.160
Observations	12	12	12	12
Pearson Correlation	0.9999		0.9995	
Hypothesized Mean Dif.	0		0	
Degrees of Freedom, df	11		11	
t Stat	8.240		8.236	
$P(T \leq t)$ one-tail	2.46E-06		2.48E-06	
t Critical one-tail	1.796		1.796	
$P(T \leq t)$ two-tail	4.93E-06		4.95E-06	
t Critical two-tail	2.201		2.201	

^aLogarithms (\log_{10}) of t_{grav} data were used in the analysis to ensure a normal distribution of the data.

has a mean equal to zero is rejected, meaning that the differences between t_{grav} values are significant. We hence strongly recommend using soil-dependent β values in future applications, whether using implicit or explicit solutions.

3.5. Application of t_{grav}

This section briefly discusses selected top-of-mind examples where the use of t_{grav} is suggested. As mentioned in the Introduction, several previous studies used t_{grav} from different perspectives. Philip (1969) himself used the parameter (denoted here as $t_{\text{grav,Philip}}$) as a priori indicator to determine the time domain validity of his TSE solution and its truncated forms. We therefore briefly explored if t_{grav} and $t_{\text{grav,Philip}}$ accurately represented the time domain validity of AAP TSE approximate expansions (which are identical to Philip's TSE approximate expansions) by analyzing 1D simulated infiltration curves obtained with HYDRUS-1D. Results are shown in Figure 9 for four soil textural classes.

As can be seen from the results in Figure 9, $t_{\text{grav,Philip}}$ was not a good time domain validity indicator for the TSE approximations. It gave a far too high value its safe use. Interestingly, Figure 9 shows that the AAP 2T equation diverged from the simulated data already at small infiltration times in nearly all cases, thus suggesting that this approximation should be used with caution, especially for late infiltration times. The 3T equation represented infiltration well, even at later times when its curve diverges from the simulated HYDRUS-1D curves. Furthermore, the reformulated t_{grav} seemed to be a good indicator for the time domain validity of the 3T equation.

As mentioned before, Ross et al. (1996) used $t_{\text{grav,Philip}}$ and $I_{\text{grav,Philip}}$ to scale times ($t^* = 2t/t_{\text{grav,Philip}}$) and the cumulative infiltration curves ($I^* = 2I/I_{\text{grav,Philip}}$) to obtain a dimensionless implicit analytical equation for infiltration. Their equation could be used to determine dimensionless parameters of the normalized soil water retention and hydraulic conductivity functions. Using reformulated t_{grav} and I_{grav} values instead of $t_{\text{grav,Philip}}$ and $I_{\text{grav,Philip}}$ to scale the infiltration data would produce different scaling factors and indirectly lead to varying predictions of the hydraulic parameters. While beyond the scope of our current study, this topic should be analyzed in future research.

We also briefly evaluated if the reformulated t_{grav} or $t_{\text{grav,Philip}}$ parameters were able to accurately represent the time to reach steady-state infiltration, as done by Reynolds et al. (2000). For this we fitted linear steady-state lines to the HYDRUS data to determine steady-state infiltration (I_{ssi}) attainment as explained in Section 2.6. The results in Figure 10 show that although t_{grav} with a value of 0.24 hr is still slightly conservative for coarse-textured soils, it served as a useful indicator for attainment of steady-state infiltration (with t_{ssi} of 0.2 hr) not captured by Philip's $t_{\text{grav,Philip}}$ value of 0.1 hr. By comparison, t_{grav} of the fine-textured soils was too conservative (much to the right of the tangent departure point), where t_{grav} (~80 hr) was almost three times the value of t_{ssi} (30 hr). In contrast, $t_{\text{grav,Philip}}$ was located to the left, indicating early times for steady-state infiltration with a $t_{\text{grav,Philip}}$ value of 26 hr. Still, it seems that times slightly beyond $t_{\text{grav,Philip}}$ would capture the time to steady-state infiltration more accurately. In case of intermediate soil textures (loam, silt, silty clay, and silty clay loam), both criteria seemed to fall beyond the time when steady state is reached (with t_{grav} and $t_{\text{grav,Philip}}$ being 5–10 times larger than t_{ssi}). Therefore, neither $t_{\text{grav,Philip}}$ nor t_{grav} would be suitable estimates for the time when steady-state infiltration will be reached. We note that t_{grav} , which defines the time during which the truncated approximate expansions of AAP TSE are valid, can serve as an indicator for the attainment of steady-state infiltration if the approximation is accurate for all times until steady state is reached (i.e., remaining valid beyond the time when steady state is reached). Figure 10 shows that $t_{\text{grav,Philip}}$ violated this condition by for fine-textured (Figure 10a) and coarse-textured (Figure 10d) soils.

Lassabatere et al. (2006) also used $t_{\text{grav,Philip}}$ in their BEST method to determine the maximum valid time, $t_{\text{max}} = 1/4(1 - B)^2 t_{\text{grav}}$ with B a constant, for transient expressions as well as for the predictions of S and K_s . Considering that the reformulated t_{grav} improves the estimation of the maximum time, using it in the BEST

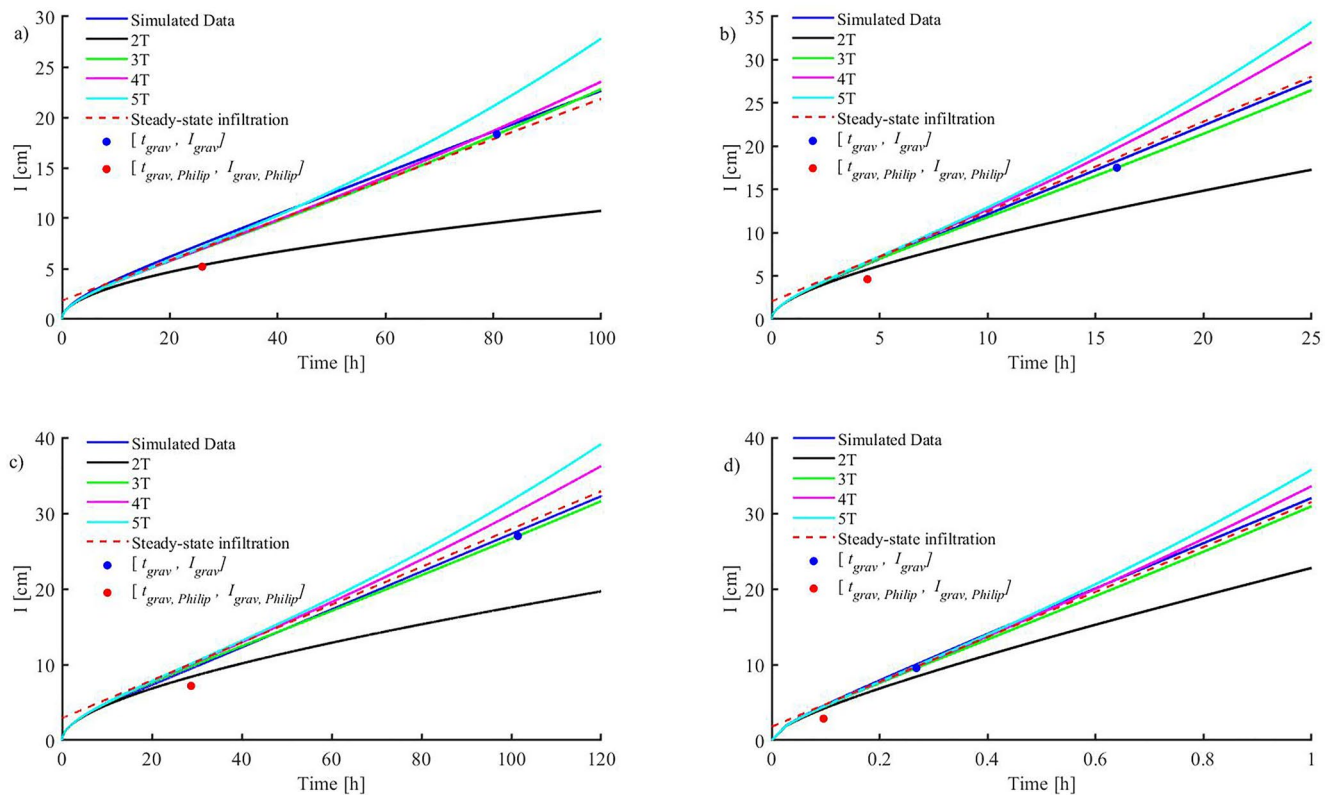


Figure 9. Simulated infiltration curves obtained with HYDRUS-1D and the approximate 2T, 3T, 4T, and 5T approximate expansions (AAP TSE) as obtained for four out of 12 USDA soil textural classes (a): clay, (b) loam, (c) silt, and (d) sand. Also shown is the steady-state infiltration curve of linear regression matched to the late-time simulation data. The red and blue dots show the relationships between time domain validity of the AAP time series expansion (TSE) and the reformulated t_{grav} and classical $t_{\text{grav,Philip}}$ characteristic times.

method may result in different results for the S and K_s predictions. Using similar concept as those presented here, Rahmati et al. (2020) also showed that inferring soil hydraulic parameters (S and K_s) from infiltration data works better when the infiltration data are measured until t_{grav} is reached. They furthermore showed that infiltration measurements for durations shorter than t_{grav} could lead to significant errors in the S and K_s predictions, particularly when estimating K_s . Their results also indicated that the infiltration measurements should be long enough for robust interpretation of real field measurements.

4. Conclusions

The seminal papers of Philip (1957, 1969) describing cumulative infiltration by a TSE is still a widely used approach to analyze the infiltration process, where water enters the soil profile via the surface. Regardless of whether the gravity time, t_{grav} , serves as a good indicator for the time domain validity of Philip's TSE expansion, it is of great interest to reformulate t_{grav} using all possible terms of the TSE, or by means of another general infiltration model that is valid for all infiltration times. This because the higher-order terms in the TSE are known to exert a significant impact on infiltration, especially at longer times where the truncated two-term equation of Philip fails to describe infiltration appropriately. On the other hand, theoretically, t_{grav} is a general concept based on equal contribution of capillarity and gravity on cumulative infiltration, that remains valid regardless of the infiltration model being used. For these reasons, we reformulated t_{grav} to be $t_{\text{grav}} = F(\beta)S^2/(K_s - K_i)^2$ using the AAP of Parlange et al. (1982), which has no time constraints. Using AAP, we were able to explore the effects of a fourth parameter (a soil specific shape parameter β) on t_{grav} in addition to S , K_s , and K_i . The effects of β on t_{grav} are implemented in the form of a functional relationship $F(\beta)$. Finally, we provided an implicit and an explicit solution for $F(\beta)$ and examined the effects of β (both constant and soil-dependent) and initial soil moisture conditions

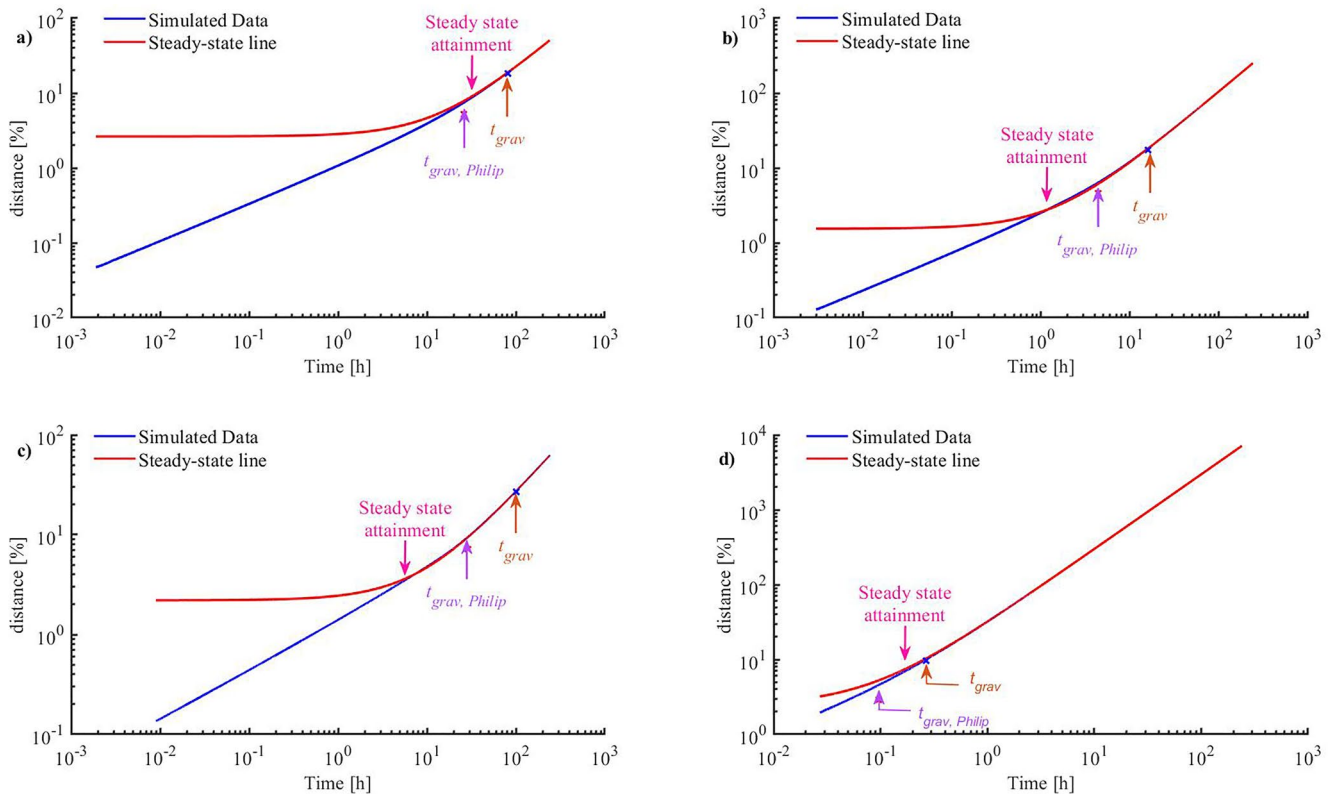


Figure 10. Relationships between the time to reach steady-state infiltration and the reformulated t_{grav} and classical $t_{\text{grav,Philip}}$ characteristic times for four out of 12 USDA soil classes (a) clay, (b) loam, (c) silt, and (d) sand. Simulated data were based on HYDRUS simulations.

on $F(\beta)$, and consequently on t_{grav} . Finally, we analyzed the use of the classical $t_{\text{grav,Philip}}$ as well as a reformulated t_{grav} on the plausibility of these two time-indicators to serve as time domain validity criteria for AAP TSE and related approximate expansions (which are assumed to be identical to Philip's TSE approximate expansions), and as a criterion for determining the time when steady state infiltration is reached. We also discussed the possible accuracy of the inferred soil hydraulic properties when classical and reformulated t_{grav} definitions are considered. Based on the results, the following conclusions can be drawn:

1. The reformulated t_{grav} is 2.59–3.25 times (3.1 on average) larger than the classical t_{grav} . The differences between the classical and reformulated t_{grav} parameters seem to be much higher in the case of fine-textured soils.
2. Practically, a linear relationship exists between $F(\beta)$ and β , with higher β values leading to higher $F(\beta)$ values.
3. The initial soil moisture content did not cause any changes in $F(\beta)$ and consequently also not in t_{grav} , thus showing that for nearly all soil saturation degrees and soil types, the term δ related to K_i can be set to zero with little or no effects on the results.
4. Finding considerable differences between the implicit and explicit solutions of $F(\beta)$, final calculations of t_{grav} also showed significant differences between the implicit and explicit solutions, particularly for intermediate soil texture classes. We therefore recommend usage of the implicit solution.
5. The use of a constant value of 0.6 for β , as suggested by Haverkamp et al. (1994), resulted in erroneous t_{grav} values compared to soil dependent β values when the explicit solution was used. This was not the case when the implicit solution was used. We therefore strongly suggest avoiding a constant β for practical implications, or to use a constant β only along with the implicit solution.
6. The reformulated t_{grav} appeared to be a better indicator for the time domain validity of Philip's TSE and the AAP 3T approximation compared to the classical $t_{\text{grav,Philip}}$.
7. The reformulated t_{grav} expressions were found to be suitable for the time when steady state infiltration is reached in coarse-textured soils. However, both classical and reformulated t_{grav} expressions performed poorly when applied to fine-textured soils, for which the reformulated t_{grav} was too conservative and $t_{\text{grav,Philip}}$ too short.

Data Availability Statement

The test data is accessible at <https://access.onlinelibrary.wiley.com/doi/10.1002/vzj2.20068>.

Acknowledgments

None.

References

- Anderson, M., Woessner, W., & Hunt, R. (2015). Spatial discretization and parameter assignment, *Applied groundwater modeling*. (pp. 181–255). Elsevier. <https://doi.org/10.1016/b978-0-08-091638-5.00005-5>
- Assouline, S., & Ben-Hur, A. (2006). Effects of rainfall intensity and slope gradient on the dynamics of interrill erosion during soil surface sealing. *Catena*, 66(3), 211–220. <https://doi.org/10.1016/j.catena.2006.02.005>
- Carsel, R. F., & Parrish, R. S. (1988). Developing joint probability-distributions of soil-water retention characteristics. *Water Resources Research*, 24(5), 755–769. <https://doi.org/10.1029/WR024i005p00755>
- Fuentes, C., Haverkamp, R., & Parlange, J. Y. (1992). Parameter constraints on closed-form soilwater relationships. *Journal of Hydrology*, 134(1–4), 117–142. [https://doi.org/10.1016/0022-1694\(92\)90032-Q](https://doi.org/10.1016/0022-1694(92)90032-Q)
- Garrote, L., & Bras, R. L. (1995). An integrated software environment for real-time use of a distributed hydrologic model. *Journal of Hydrology*, 167(1–4), 307–326. [https://doi.org/10.1016/0022-1694\(94\)02593-Z](https://doi.org/10.1016/0022-1694(94)02593-Z)
- Haverkamp, R., Ross, P., Smettem, K., & Parlange, J. (1994). Three-dimensional analysis of infiltration from the disc infiltrometer: 2. Physically based infiltration equation. *Water Resources Research*, 30(11), 2931–2935. <https://doi.org/10.1029/94WR01788>
- Iverson, R. M. (2000). Landslide triggering by rain infiltration. *Water resources research*, 36(7), 1897–1910. <https://doi.org/10.1029/2000WR900090>
- Kim, D., Ray, R. L., & Choi, M. (2017). Simulations of energy balance components at snow-dominated montane watershed by land surface models. *Environmental Earth Sciences*, 76(9), 337. <https://doi.org/10.1007/s12665-017-6655-0>
- Kutílek, M., & Krejca, M. (1987). Three-parameter infiltration equation of Philip type. *Vodohosp. cas*, 35, 52–61.
- Lassabatere, L., Angulo-Jaramillo, R., Soria-Ugalde, J. M., Simunek, J., & Haverkamp, R. (2009). Numerical evaluation of a set of analytical infiltration equations. *Water Resources Research*, 45(12). <https://doi.org/10.1029/2009wr007941>
- Lassabatere, L., Angulo-Jaramillo, R., Ugalde, J. M. S., Cuenca, R., Braud, I., & Haverkamp, R. (2006). Beerkan estimation of soil transfer parameters through infiltration experiments - BEST. *Soil Science Society of America Journal*, 70(2), 521–532. <https://doi.org/10.2136/sssaj2005.0026>
- Lassabatere, L., Peyneau, P.-E., Yilmaz, D., Pollacco, J., Fernández-Gálvez, J., Latorre, B., et al. (2021). A scaling procedure for straightforward computation of sorptivity. *Hydrology and Earth System Sciences*, 25(9), 5083–5104. <https://doi.org/10.5194/hess-25-5083-2021>
- Latorre, B., Moret-Fernández, D., Lassabatere, L., Rahmati, M., López, M., Angulo-Jaramillo, R., et al. (2018). Influence of the β parameter of the Haverkamp model on the transient soil water infiltration curve. *Journal of Hydrology*, 564, 222–229. <https://doi.org/10.1016/j.jhydrol.2018.07.006>
- Lehmann, P., & Or, D. (2012). Hydromechanical triggering of landslides: From progressive local failures to mass release. *Water Resources Research*, 48(3). <https://doi.org/10.1029/2011wr010947>
- MacDonald, M. K., Pomeroy, J. W., & Essery, R. L. H. (2018). Water and energy fluxes over northern prairies as affected by chinook winds and winter precipitation. *Agricultural and Forest Meteorology*, 248, 372–385. <https://doi.org/10.1016/j.agrformet.2017.10.025>
- Moret-Fernández, D., Latorre, B., López, M. V., Pueyo, Y., Lassabatere, L., Angulo-Jaramillo, R., et al. (2020). Three-and four-term approximate expansions of the Haverkamp formulation to estimate soil hydraulic properties from disc infiltrometer measurements. *Hydrological Processes*, 34(26), 5543–5556. <https://doi.org/10.1002/hyp.13966>
- Mualem, Y. (1976). A new model for predicting the hydraulic conductivity of unsaturated porous media. *Water resources research*, 12(3), 513–522. <https://doi.org/10.1029/WR012i003p00513>
- Parlange, J.-Y., Lisle, I., Braddock, R., & Smith, R. (1982). The three-parameter infiltration equation. *Soil Science*, 133(6), 337–341. <https://doi.org/10.1097/00010694-198206000-00001>
- Philip, J. (1957). The theory of infiltration: 1. The infiltration equation and its solution. *Soil Science*, 83(5), 345–358. <https://doi.org/10.1097/00010694-195705000-00002>
- Philip, J., & Farrell, D. (1964). General solution of the infiltration-advance problem in irrigation hydraulics. *Journal of Geophysical Research*, 69(4), 621–631. <https://doi.org/10.1029/jz069i004p00621>
- Philip, J. R. (1957). The theory of infiltration: 4. Sorptivity and algebraic infiltration equations. *Soil Science*, 84(3), 257–264. <https://doi.org/10.1097/00010694-195709000-00010>
- Philip, J. R. (1969). Theory of infiltration. *Advances in Hydrosceince*, 5, 215–296. <https://doi.org/10.1016/B978-1-4831-9936-8.50010-6>
- Poesen, J., & Valentin, C. (2003). Gully erosion and global change - Preface. *Catena*, 50(2–4), 87–89. [https://doi.org/10.1016/S0341-8162\(02\)00146-7](https://doi.org/10.1016/S0341-8162(02)00146-7)
- Rahmati, M., Latorre, B., Lassabatere, L., Angulo-Jaramillo, R., & Moret-Fernandez, D. (2019). The relevance of Philip theory to Haverkamp quasi-exact implicit analytical formulation and its uses to predict soil hydraulic properties. *Journal of Hydrology*, 570, 816–826. <https://doi.org/10.1016/j.jhydrol.2019.01.038>
- Rahmati, M., Rezaei, M., Lassabatere, L., Morbidelli, R., & Vereecken, H. (2021). Simplified characteristic time method for accurate estimation of the soil hydraulic parameters from one-dimensional infiltration experiments. *Vadose Zone Journal*, 20(3), e20117. <https://doi.org/10.1002/vzj2.20117>
- Rahmati, M., Vanderborght, J., Simunek, J., Vrugt, J. A., Moret-Fernandez, D., Latorre, B., et al. (2020). Soil hydraulic properties estimation from one-dimensional infiltration experiments using characteristic time concept. *Vadose Zone Journal*, 19(1), e20068. <https://doi.org/10.1002/vzj2.20068>
- Reynolds, W. D., Bowman, B. T., Brunke, R. R., Drury, C. F., & Tan, C. S. (2000). Comparison of tension infiltrometer, pressure infiltrometer, and soil core estimates of saturated hydraulic conductivity. *Soil Science Society of America Journal*, 64(2), 478–484. <https://doi.org/10.2136/sssaj2000.642478x>
- Richards, L. A. (1931). Capillary conduction of liquids through porous mediums. *Physics—A Journal of General and Applied Physics*, 1(1), 318–333. <https://doi.org/10.1063/1.1745010>
- Ross, P. J., Haverkamp, R., & Parlange, J. Y. (1996). Calculating parameters for infiltration equations from soil hydraulic functions. *Transport in Porous Media*, 24(3), 315–339. <https://doi.org/10.1007/Bf00154096>
- Šimunek, J., Genuchten, M. T., & Šejna, M. (2008). Development and applications of the HYDRUS and STANMOD software packages and related codes. *Vadose Zone Journal*, 7(2), 587–600. <https://doi.org/10.2136/vzj2007.0077>

- Šimůnek, J., Van Genuchten, M. T., & Šejna, M. (2016). Recent developments and applications of the HYDRUS computer software packages. *Vadose Zone Journal*, 15(7), vzj2016. <https://doi.org/10.2136/vzj2016.04.0033>
- Van Genuchten, M. T. (1980). A closed-form equation for predicting the hydraulic conductivity of unsaturated soils. *Soil Science Society of America Journal*, 44(5), 892–898. <https://doi.org/10.2136/SSSAJ1980.03615995004400050002X>
- Varado, N., Braud, I., Ross, P. J., & Haverkamp, R. (2006). Assessment of an efficient numerical solution of the 1D Richards' equation on bare soil. *Journal of Hydrology*, 323(1–4), 244–257. <https://doi.org/10.1016/j.jhydrol.2005.07.052>
- Vereecken, H., Weihermüller, L., Assouline, S., Šimůnek, J., Verhoef, A., Herbst, M., et al. (2019). Infiltration from the pedon to global grid scales: An overview and outlook for land surface modeling. *Vadose Zone Journal*, 18(1), 1–53. <https://doi.org/10.2136/vzj2018.10.0191>
- Verhoef, A., & Egea, G. (2013). Soil water and its management. In G. Peter J., & N. Stephen (Eds.), *Soil conditions and plant growth* (pp. 269–322). <https://doi.org/10.1002/9781118337295.ch9>
- Villeneuve, S., Cook, P. G., Shanafield, M., Wood, C., & White, N. (2015). Groundwater recharge via infiltration through an ephemeral riverbed, central Australia. *Journal of Arid Environments*, 117, 47–58. <https://doi.org/10.1016/j.jaridenv.2015.02.009>
- Waechter, R., & Philip, J. (1985). Steady two- and three-dimensional flows in unsaturated soil: The scattering analog. *Water Resources Research*, 21(12), 1875–1887. <https://doi.org/10.1029/WR021i012p01875>